


Original Research

Aldosterone-Induced Renal Lymphangiogenesis and Endothelial-To-Mesenchymal Transformation to Promote Renal Interstitial Fibrosis Through the MR/TGF- β 1 Pathway in Mice

Lili Fan^{1,2,†}, Ziqian Liu^{1,3,†}, Yi Chang^{1,4}, Yunzhao Xiong^{1,4}, Fan Yang^{1,4}, Xiaomeng Gao¹, Jingyue Chang¹, Tatsuo Shimosawa⁵, Qingyou Xu^{1,4,*}, Panpan Qiang^{1,4,*} 

¹Hebei Key Laboratory of Integrative Medicine on Liver-Kidney Patterns, Hebei University of Chinese Medicine, 050200 Shijiazhuang, Hebei, China

²Department of Nephrology, Chuzhou Integrated Traditional Chinese and Western Medicine Hospital, 239054 Chuzhou, Anhui, China

³Department of Pharmacy and Health Management, Hebei Chemical & Pharmaceutical College, 050026 Shijiazhuang, Hebei, China

⁴Institute of Integrative Medicine, College of Integrative Medicine, Hebei University of Chinese Medicine, 050200 Shijiazhuang, Hebei, China

⁵Department of Clinical Laboratory, School of Medicine, International University of Health and Welfare, 286-8686 Narita, Japan

*Correspondence: qingyouxu@hebcm.edu.cn (Qingyou Xu); qiangpanpan@hebcm.edu.cn (Panpan Qiang)

†These authors contributed equally.

Academic Editors: Moo-Ho Won and Guoping Zheng

Submitted: 6 August 2025 Revised: 4 October 2025 Accepted: 31 October 2025 Published: 27 November 2025

Abstract

Background: Lymphangiogenesis and phenotypic transformation of endothelial cells are closely associated with the progression of renal interstitial fibrosis. Inflammatory injury triggered by mineralocorticoid receptor (MR) activation serves as the initial stimulus for lymphangiogenesis. **Methods:** Thirty specific pathogen-free (SPF) male C57BL/6 mice were assigned to three groups randomly: the control group (CON), aldosterone-treated group (ALD group, in which aldosterone was infused at a rate of 0.75 μ g/h via mini-osmotic pumps for 12 weeks), and esaxerenone-treated group (ESA group, administered at a dosage of 1 mg/kg/day via diet). The expression levels of lymphatic markers (lymphatic vessel endothelial hyaluronan receptor 1 (LYVE-1), vascular endothelial growth factor receptor 3 (VEGFR3), podoplanin, and VEGFC) were assessed using immunohistochemistry, immunofluorescence, and western blot analysis. Inflammatory injury markers (CD68, F4/80, IL-1 β , TNF- α and TGF- β 1) and endothelial-to-mesenchymal transition (EndMT, LYVE-1⁺ vimentin/ α smooth muscle actin (α -SMA)⁺) were evaluated. *In vitro*, the effects of aldosterone on the migration, tube formation, and phenotypic transformation of human lymphatic endothelial cells (HLECs) in the presence of TGF- β 1 or VEGFC were investigated. **Results:** In the ALD group, significant increases in lymphangiogenesis, macrophage infiltration, and the expression of TGF- β 1, TNF- α , IL-1 β and VEGFC were observed. Immunofluorescence double staining revealed that VEGFC was predominantly secreted by macrophages, and that lymphatic endothelial cells exhibited expression of vimentin and α -SMA. *In vitro* experiments demonstrated that aldosterone promoted HLECs migration and tube formation, as well as the activation of inflammatory cytokines and MR. Flow cytometry analysis indicated that HLECs underwent myofibroblastic transformation, which could be attenuated by MR blocker esaxerenone. **Conclusions:** Aldosterone induces inflammatory injury, thereby promoting renal lymphangiogenesis and EndMT.

Keywords: aldosterone; mineralocorticoid receptor; VEGFC; lymphangiogenesis; TGF- β 1; EndMT

1. Introduction

Chronic kidney disease (CKD) is defined as the presence of abnormalities in kidney structure or function that cause health consequences [1]. Renal interstitial fibrosis (RIF) is a common pathological finding and the ultimate manifestation of CKD [2]. RIF is characterized by abnormal deposition of extracellular matrix and organ atrophy, and is related to cell proliferation, apoptosis, and phenotypic transformation. Clinical and animal experiments have shown that aberrant angiogenesis and lymphangiogenesis, especially inflammatory lymphangiogenesis, are involved in RIF [3]. Renal biopsy samples from patients with IgA nephropathy and diabetic kidney disease were labeled with the human lymphatic vessel endothelial marker D2-40, and these samples exhibited a significantly increased number of lymphatic drainage vessels, moreover, both the quantity of

lymphatics and the severity of RIF and inflammation were positively correlated, and some lymphatic vessel endothelial cells underwent myofibroblast-like transformation, secreted α smooth muscle actin (α -SMA), and were involved in the development of renal fibrosis [4]. During renal transplant rejection, the number of lymphatic vessels also increased significantly and was accompanied by the infiltration of many inflammatory cells [3]. In animal experiments, long-term (180 d) unilateral ureteral obstruction (UUO) can mediate the formation of lymphatic vessels in the contralateral kidney, and the administration of eplerenone, a mineralocorticoid receptor blocker (MRB), prevents the progression of fibrosis [5].

Lymphangiogenesis is regulated by vascular endothelial growth factors (VEGFs) of which VEGFC and VEGFD are the most important. In particular, VEGFC is a key fac-



tor in lymphangiogenesis. Renal VEGFC can be secreted by a variety of renal cells under physiological conditions, such as renal tubular epithelial cells, mesangial cells, vascular endothelial cells and fibroblasts under physiological conditions, with renal tubular epithelial cells serving as the predominant source. But during inflammatory injury, macrophages oversecrete VEGFC [6].

Aldosterone is well known to induce inflammatory and profibrotic factors that cause kidney injury via activation of the mineralocorticoid receptor (MR) [7]. Previous studies have shown that aldosterone can induce renal injury with abnormal neovascularization which is involved in fibrosis formation, mainly mediated by VEGFA [8]. In this study, we also reported that inflammatory lymphangiogenesis was associated with this process, and inflammatory cells, especially macrophages, secreted VEGFC to promote lymphangiogenesis. Additionally, the increase in lymphatic vessels led to disorganization of the renal structure, while phenotypic transformation of lymphatic endothelial cells was also involved in this process with aldosterone-infused group (ALD), a mineralocorticoid that induces inflammatory damage. Whether aldosterone stimulates renal lymphangiogenesis or participates in renal fibrosis remains unknown. In this study, mice were continuously administered aldosterone to induce MR-mediated inflammatory lymphangiogenesis and endothelial-to-mesenchymal transition (EndMT) through the VEGFC and TGF- β 1 pathways, and the protective effects of esaxerenone as an MRB were evaluated.

2. Materials and Methods

2.1 Animals and Study Design

The animal study was approved by the Ethics Committee of Hebei University of Chinese Medicine. Thirty specific pathogen-free (SPF) male C57BL/6 mice, weighing 24.7 ± 1.1 g and aged 6–8 weeks, were provided by Liaoning Changsheng Biotechnology Co., Ltd., Changchun, China. The mice were maintained under a 12-hour light/dark cycle at a controlled ambient temperature of 25 °C, with ad libitum access to standard rodent chow and tap water. All animal care and experimental procedures were conducted in accordance with the guidelines provided by the Animal Experimentation Ethics Committee of Hebei University of Chinese Medicine and were approved by the Animal Care and Use Committee of the same institution. All efforts were made to minimize animal distress and ensure ethical treatment.

Thirty mice were divided randomly into 3 groups: the control (CON) group, the ALD group (The mice were received continuous ALD infusion at 0.75 μ g/h via a miniosmotic pump and the pumps were replaced every 6 weeks for the entire duration of the study; CAS NO: 52-39-1, Cayman Chemical, Ann Arbor, MI, USA), and the esaxerenone-treated group (ESA group) (aldosterone infusion + esaxerenone administration via diet at a dosage of 1

mg/kg/day, kindly provided by Daiichi Sankyo Co., Ltd., Tokyo, Japan). The mice were acclimatized and fed for 7 days before modeling. The mice were anesthetized via chamber induction with 4% isoflurane in 100% oxygen (1 L/min) until loss of righting reflex. Surgical anesthesia was maintained via nose cone with 1.5–2% isoflurane in oxygen (0.5 L/min), confirmed by absent pedal reflex and stable respiration. The modeling method has been described previously [8]. After twelve weeks, animals were initially anesthetized with a low concentration of isoflurane, followed by a rapid transition to a high concentration (5%) to induce immediate loss of consciousness, after which kidney tissue samples and blood were collected.

2.2 Histological Analysis and Immunohistochemical Staining

Renal pathological specimens were obtained as previously described [8]. Hematoxylin and eosin (H&E) staining, Masson staining, and immunohistochemistry were performed with antibodies against F4/80 (1:100; Servicebio, Wuhan, China, Cat# GB113373), CD68 (1:100, Abcam, Cambridge, UK, Cat# ab53444), α -SMA (1:100, Servicebio, Cat# GB13044), vimentin (1:100, Abcam, Cat# ab92547), lymphatic vessel endothelial hyaluronan receptor 1 (LYVE-1) (1:50, Novus, Centennial, CO, USA; Cat# NB600-1008), podoplanin (1:50, Bioss, Woburn, MA, USA, Cat# bs-1048R), vascular endothelial growth factor receptor-3 (VEGFR3) (1:50, Abcam, Cat# ab27278), type III collagen (COL III) (1:100, Abcam, Cat# ab283694), IL-1 β (1:100, Abcam, Cat# ab283822), TNF- α (1:100, Abcam, Cat# ab307164), TGF- β 1 (1:100, Abcam, Cat# ab215715), and VEGFC (1:100, Immunoway, Plano, TX, USA, Cat# Y75297). The sections were viewed under a Leica inverted microscope (DMI6000-CS; Leica Microsystems, Wetzlar, Germany). A Leica TCS SP8 instrument equipped with LAS AF software was used for observation and imaging.

On H&E-stained slides, inflammatory cell infiltration and tubulointerstitial changes were graded semiquantitatively by two investigators in a blinded fashion. A 0–6 scoring scale was used to evaluate the two items, where scores of 0, 1, 2, and 3 represented normal, mild, moderate, and severe conditions, respectively [9]. The percentage of the collagen positive area was semiquantitatively graded by Masson staining. The images were analyzed using ImageJ software (National Institutes of Health, Bethesda, MD, USA).

2.3 Immunofluorescence Analysis

The kidneys were perfused with saline, and dehydrated in 20% and 30% sucrose solutions, and the OCT complex was frozen for immunofluorescence staining (Sakura, Torrance, CA, USA). After being taken from the frozen samples, 6 μ m kidney sections were stained with Alexa Fluor 555-coupled α -SMA (1:300, Abcam,

Cat# ab175651) or the following noncoupled antibodies for staining: anti-LYVE-1 (1:50, Novus, Cat# NB600–1008), vimentin (1:100, Affinity, Nottingham, UK, Cat# BF8006), COL III (1:100, Abcam, Cat# ab283694), anti-VEGFC (1:100, Immunoway, Cat# Y75297), and anti-F4/80 (1:100, Servicebio, Cat# GB113373). Second or third fluorescence staining of the sections was performed. After sections were stained, nuclei were stained with or without DAPI, sealed and photographed for observation under a confocal microscope (CTS SP8, Leica Microsystems, Wetzlar, Germany).

2.4 Protein Extraction and Protein Blot Analysis

Kidney tissues, RAW264.7 cells, and human lymphatic endothelial cells (HLECs) were homogenized in radioimmunoprecipitation assay (RIPA) buffer containing protease inhibitors, and total protein was extracted. Protein samples were separated by 10% sodium dodecyl sulfate-polyacrylamide gel electrophoresis (SDS–PAGE) and then transferred to polyvinylidene fluoride (PVDF) membranes. After blocking with 5% skim milk at room temperature for 2 h, the membranes were incubated with the following primary antibodies at 4 °C overnight: vimentin (1:1000, Abcam, Cat# ab8978), IL-1 β (1:300, Abcam, Cat# ab283822), IL-1 β (1:500, Affinity, Cat# AF5103), TGF- β 1 (1:1000, Abcam, Cat# ab215715), VEGFR3 (1:500, Abcam, Cat# ab27278), α -SMA (1:1000, ABclonal, Wuhan, China, Cat# A17910), TNF- α (1:1000, ABclonal, Cat# A0277), podoplanin (1:1000, ABclonal, Cat# A13261), LYVE-1 (1:1000, ABclonal, A4352), VEGFC (1:1000, Immunoway, Cat# Y75297), and NR3C2 (1:300, Proteintech, Wuhan, China, Cat# 21854-1-AP). On the second day, the membrane was incubated with a secondary antibody (1:10,000) at room temperature for 1 h. Odyssey imaging system (LI-COR system, Lincoln, NE, USA) or e-BLOT system (Shanghai e-BLOT Photoelectrics Technology Co., Ltd., Shanghai, China) was used to detect the protein bands, determination of target protein bands with ImageJ software (National Institutes of Health) relative to the housekeeping protein such as GAPDH (1:1000, Affinity, Cat# T0004), β -actin (1:1000, Affinity, Cat# T0022), β -Tubulin (1:1000, Affinity, Cat# T0023), or PCNA bands (1:1000, Proteintech, Cat# 10205-2-AP).

2.5 In Vitro Cell Culture Assay

RAW264.7 (Cat# CL-0190, Procell Life Science and Technology Co., Ltd., Wuhan, China) was cultured as previously described [10]. HLECs (Cat# HUM-CELL-0053, PriCells, Wuhan, China) were cultured in endothelial cell medium (ECM, ScienCell, Carlsbad, CA, USA) supplemented with 10% FBS, 1% endothelial cell growth supplement (ECGS) and 1% penicillin and streptomycin. The cells were maintained at 37 °C in a humidified atmosphere of 5% CO₂. All the cell lines were validated by STR profiling and tested negative for mycoplasma.

RAW264.7 cells were divided into 3 groups: the CON group, ALD group (treated with 10^{−7} mol/L ALD for 24 h), and ESA group (treated with 10^{−6} mol/L esaxerenone 2 h before aldosterone treatment). HLECs were divided into 6 groups: the CON group, the ALD group (treated with 10^{−7} mol/L aldosterone for 24 h), the ESA group (treated with 10^{−6} mol/L esaxerenone 2 h before aldosterone treatment), the TGF- β 1 group (10 ng/mL administered for 24 h; MCE, Shanghai, China, Cat# HY-P70543), the TGF- β 1+LY2109761 group (TGF- β 1 inhibitor; cells were treated with 2 \times 10^{−6} mol/L LY2109761 2 h before TGF- β 1 treatment, MCE, Shanghai, China, Cat# HY-12075/CS-0571), and the ALD+LY2109761 group (pretreated with 2 \times 10^{−6} mol/L LY2109761 2 h before aldosterone treatment). In these experiments, the cells were divided into the CON group, the ALD group, the ESA group, the VEGFC group (MCE, Shanghai, China, Cat#: HY-P7313, 100 ng/mL was administered for 24 h), the VEGFC+VEGFR-3-IN-1 group (MCE, Shanghai, China, Cat#: HY-132305/CS-0200376, VEGFC receptor blocker, cells were treated with 10^{−7} mol/L VEGFR-3-IN-1 2 h prior to VEGFC treatment), and the ALD+VEGFR-3-IN-1 group (cells were pretreated with 10^{−7} mol/L VEGFR-3-IN-1 2 h before aldosterone treatment). In addition, RAW264.7, rat kidney fibroblasts (RKF; Cat#: RAT-iCELL-u014, Cellverse Bioscience Technology Co., Ltd., Shanghai, China), distal convoluted tubule cells (DCT; Cat#: CRL-3250, American Type Culture Collection, Manassas, VA, USA), and Human Kidney-2 cell (HK-2; Cat#: CL-0109, Procell Life Science & Technology, Wuhan, China) cells were stimulated with 10^{−7} mol/L aldosterone for 24 hours, after which VEGFC expression was detected by Western blot.

2.5.1 Enzyme-Linked Immunosorbent Assay (ELISA)

The processed RAW264.7 cell culture medium was centrifuged, and the supernatant was collected for subsequent experiments, which were performed using a quantitative sandwich enzyme immunoassay technique. Subsequently, 100 μ L of the supernatant was added to a microtiter plate, and the corresponding diluted antibodies (VEGFC: CUSABIO, Wuhan, China, Cat#: CSB-E07361m; TGF- β 1: Servicebio, Cat#: GEM0051; TNF- α : Servicebio, Cat#: GEM0004; and IL-1 β : Servicebio, Cat#: GEM0002) were added to the plate at room temperature for 2 h. The membrane was subsequently washed, the corresponding HRP-labeled secondary antibody was added, the plate was incubated at room temperature for 1 h followed by washing. A chromogenic substrate was added to the appropriate color development solution, and the absorbance was measured at 450 nm.

2.5.2 CCK8 Assay

A cell counting kit-8 (CCK8) assay (Abbkina, Wuhan, China, Cat# BMU106-CN) was performed according to the protocol. HLECs were divided into the CON,

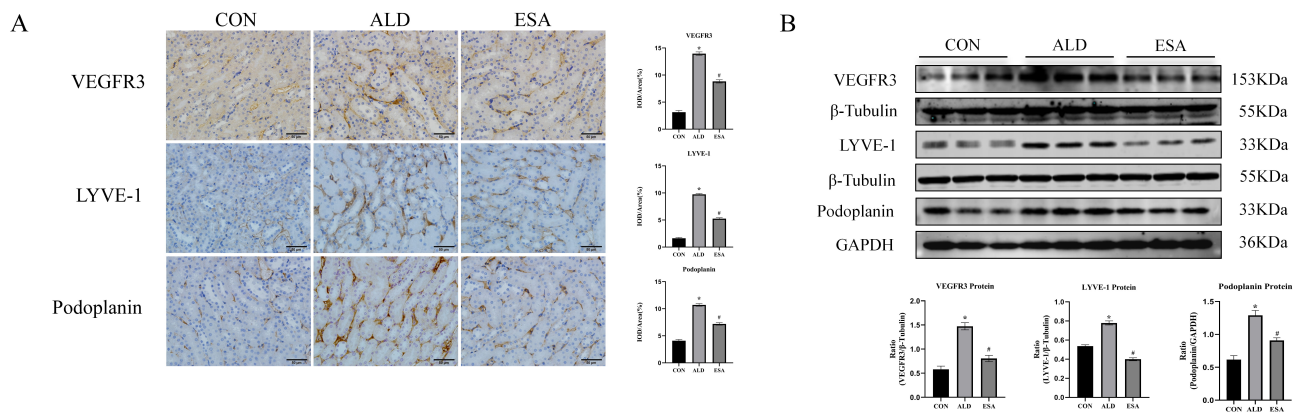


Fig. 1. Aldosterone induces renal lymphangiogenesis in mice. (A) Immunohistochemical staining was performed with anti-VEGFR3, LYVE-1, and Podoplanin antibodies to label lymphatic vessels (scale bar = 50 μ m). (B) Western blotting was performed to analyze VEGFR3, LYVE-1, and Podoplanin in renal tissues. The data are expressed as the mean \pm standard deviation (n = 6). * p < 0.05 vs. the CON group, # p < 0.05 vs. the ALD group. VEGFR3, vascular endothelial growth factor receptor-3; LYVE-1, lymphatic vessel endothelial hyaluronan receptor 1; CON, control; ALD, aldosterone.

ALD, ALD+ESA, VEGFC, VEGFC+VEGFR-3-IN-1, and ALD+VEGFR-3-IN-1 groups. HLECs were inoculated into 96-well plates (1×10^4 cells/well). Following 24 h of stimulation, 10 μ L of CCK8 solution was added per well for 4 h of incubation, after which the absorbance at 450 nm was detected using an AVersaMax microplate reader (Molecular Devices, Sunnyvale, CA, USA).

2.5.3 Scratch Wound Assay

HLECs were inoculated into 6 cm dishes and cultured to confluence. Next, a scratched was created in the center of the confluent cells with a 200 μ L pipette tip. After the cells were rinsed three times with PBS, an appropriate amount of complete medium was added. Images were acquired at 0 h and 8 h and quantified using ImageJ software (National Institutes of Health).

2.5.4 Endothelial Tube Formation Assay

Matrigel matrix (300 μ L per well; BD Biocoat 356234, Corning Inc., Corning, NY, USA) was added to precooled 12-well plates, which were then polymerized for 30 min at 37 $^{\circ}$ C. Following a 24-hour treatment period, HLECs were resuspended in 300 μ L of growth medium supplemented with 10% FBS and seeded onto the gelled Matrigel. After 3.5 h of standard incubation, tube formation was examined and photographed under a $\times 10$ objective.

2.5.5 Flow Cytometry

Twenty-four hours after treatment, the HLECs were harvested and stained with PE-conjugated anti-VEGFR3 (1:100, Biolegend, Cat# 356204), APC-conjugated anti- α -SMA (1:1000, Abcam, Cat# ab202296), and APC-conjugated anti-vimentin (1:100, Invitrogen, Waltham, MA, USA, Cat# YF3938885) antibodies. After the antibodies were added, the mixture was gently vortexed, the

flow tube was wrapped with aluminum foil to protect it from light, and the mixture was incubated at room temperature for 60 minutes. Unstained cells were used as negative controls. The cells were analyzed using a BD FACSaria II flow cytometer (BD Biosciences, Franklin Lakes, NJ, USA), viable singlet cells were selected by FSC/SSC gating, and the data were analyzed using FlowJo software (version 10, BD Biosciences, Franklin Lakes, NJ, USA).

2.6 Statistical Analysis

Statistical analyses were conducted using SPSS statistics software (version 26.0, IBM, Armonk, NY, USA). After normality assessment of the data via the Shapiro-Wilk test, one-way ANOVA was performed followed by a least significant difference test for multiple groups. The data are presented as the means \pm standard deviations (SDs). Statistical significance was defined as a p -value < 0.05.

3. Results

3.1 Aldosterone Induces Renal Lymphangiogenesis in Mice

LYVE-1, Podoplanin, and VEGFR3 are markers of lymphatic endothelial cells. Immunohistochemical staining of the kidneys of mice treated with aldosterone at 12 weeks revealed that renal interstitial lymphatic vessel markers were significantly increased and that lymphangiogenesis was significantly reduced after esaxerenone treatment (Fig. 1A). The levels of VEGFR3, LYVE-1, and Podoplanin in renal tissues (determined by Western blot of the whole kidney) reinforced the results of immunohistochemical staining (Fig. 1B). In addition, in the 12-week aldosterone-treated mouse model, H&E staining showed pathologic changes in the kidneys of aldosterone-treated mice, and Masson staining showed that the aldosterone-treated mice had significantly more renal collagen deposition than the control mice (Supplementary Fig. 1).

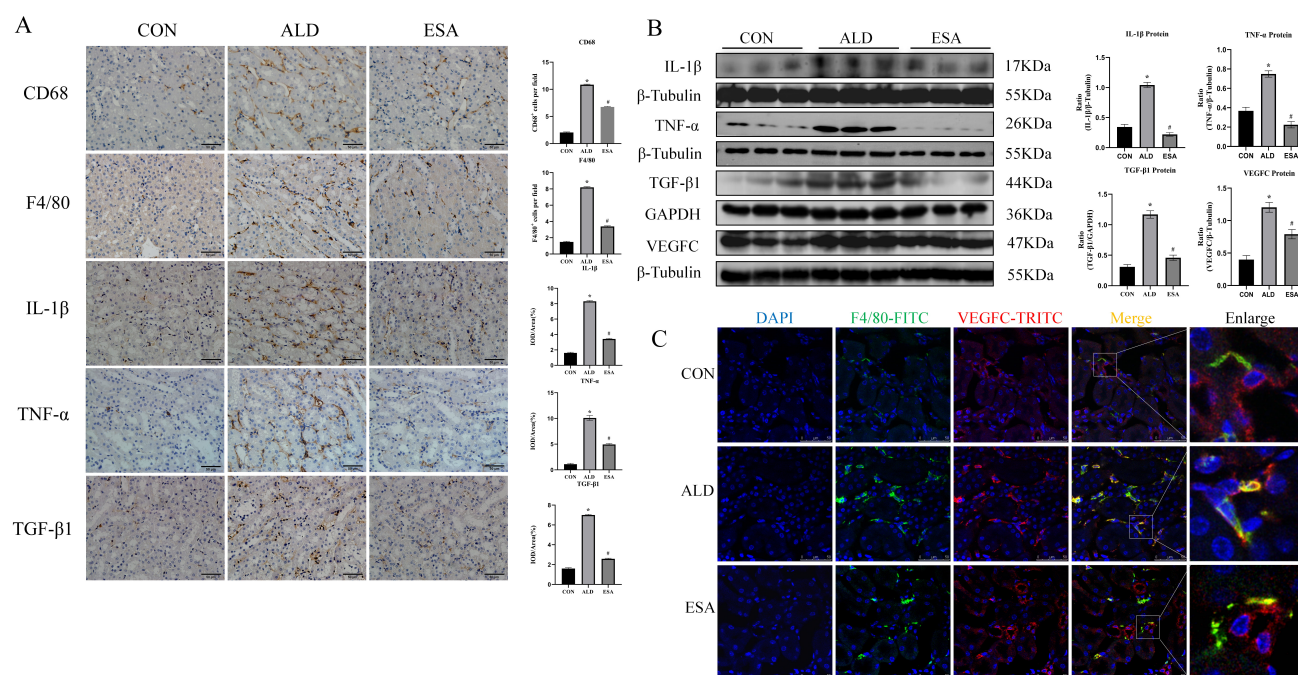


Fig. 2. Aldosterone stimulates the infiltration of macrophage and the secretion of inflammatory cytokines, VEGFC and TGF- β 1 in mice. (A) Immunohistochemical staining was performed to detect macrophages, inflammatory cytokines, and TGF- β 1 using anti-CD68, anti-F4/80, anti-TNF- α , anti-IL-1 β , anti-TGF- β 1, and anti-VEGFC antibodies (scale bar = 50 μ m). (B) Western blotting was performed to analyze the protein levels of IL-1 β , TNF- α , TGF- β 1, and VEGFC in renal tissue. (C) Immunofluorescence staining of kidney sections with anti-F4/80 antibody (green) and anti-VEGFC antibody (red) was performed to study the relationship between macrophages and VEGFC. The cell nuclei (blue) were stained with DAPI (scale bar = 50 μ m). Enlarged images showed a 5 \times magnification of the areas within the white rectangles in the merged images. The data are expressed as the mean \pm standard deviation ($n = 6$). * $p < 0.05$ vs. the CON group, # $p < 0.05$ vs. the ALD group.

3.2 Aldosterone Stimulates Macrophages to Secrete VEGFC and Inflammatory Cytokines to Stimulate the Proliferation, Migration, and Tube Formation of HLECs

The classical pathway for lymphangiogenesis is the VEGFC/VEGFR3 signaling pathway, and VEGFC is produced primarily by renal tubular cells and macrophages [11,12]. Aldosterone-treated mice exhibited abundant infiltration of macrophages labeled with F4/80 or CD68 which was inhibited by esaxerenone (Fig. 2A). Aldosterone can induce inflammatory macrophage infiltration and the secretion of inflammatory cytokines and growth factors, which mediate the inflammatory response and lead to tissue damage [13]. Immunohistochemical staining and western blot for TNF- α , IL-1 β , TGF- β 1 and VEGFC revealed that the levels of these cytokines were significantly greater in the ALD group than in the CON group, and these effects were mitigated by esaxerenone treatment. The expression of VEGFC was predominantly observed in the distal tubules in the CON group and was significantly upregulated following aldosterone treatment, particularly in the tubulointerstitial infiltrating cells (Fig. 2A,B). Next, we studied the origin of VEGFC in relation to macrophages. Immunofluorescence labeling of renal tissue for F4/80 and VEGFC revealed that the renal mesenchyme in the ALD group had

significantly more F4/80⁺VEGFC⁺ cells compared with the other groups, suggesting that aldosterone promotes the secretion of VEGFC by macrophages. The number of double-positive cells was markedly reduced by treatment with esaxerenone (Fig. 2C). In addition, western blot was also used to detect the expression of VEGFC in RAW264.7, RKF, DCT and HK-2 cells treated with aldosterone (10^{-7} mol/L aldosterone for 24 h), and the results revealed that the expression of VEGFC in these cells was upregulated after induction with aldosterone (Supplementary Fig. 2). These results indicated that VEGFC could be secreted by a variety of cells, such as renal tubular epithelial cells, fibroblasts, and especially macrophages, in aldosterone-treated mice.

To further investigate the roles of aldosterone and VEGFC in lymphangiogenesis, HLECs were cultured for 24 h with aldosterone and the inhibitor esaxerenone, VEGFC and the inhibitor VEGFR-3-IN-1, or aldosterone+VEGFR-3-IN-1. Cell proliferation was assessed with a CCK8 assay. The proliferation of HLECs in the aldosterone and VEGFC treated groups was markedly greater than that in CON group (Fig. 3A). To further investigate whether aldosterone could promote the secretion of VEGFC by HLECs, we then detected the expression of VEGFC in HLECs stimulated with aldosterone through

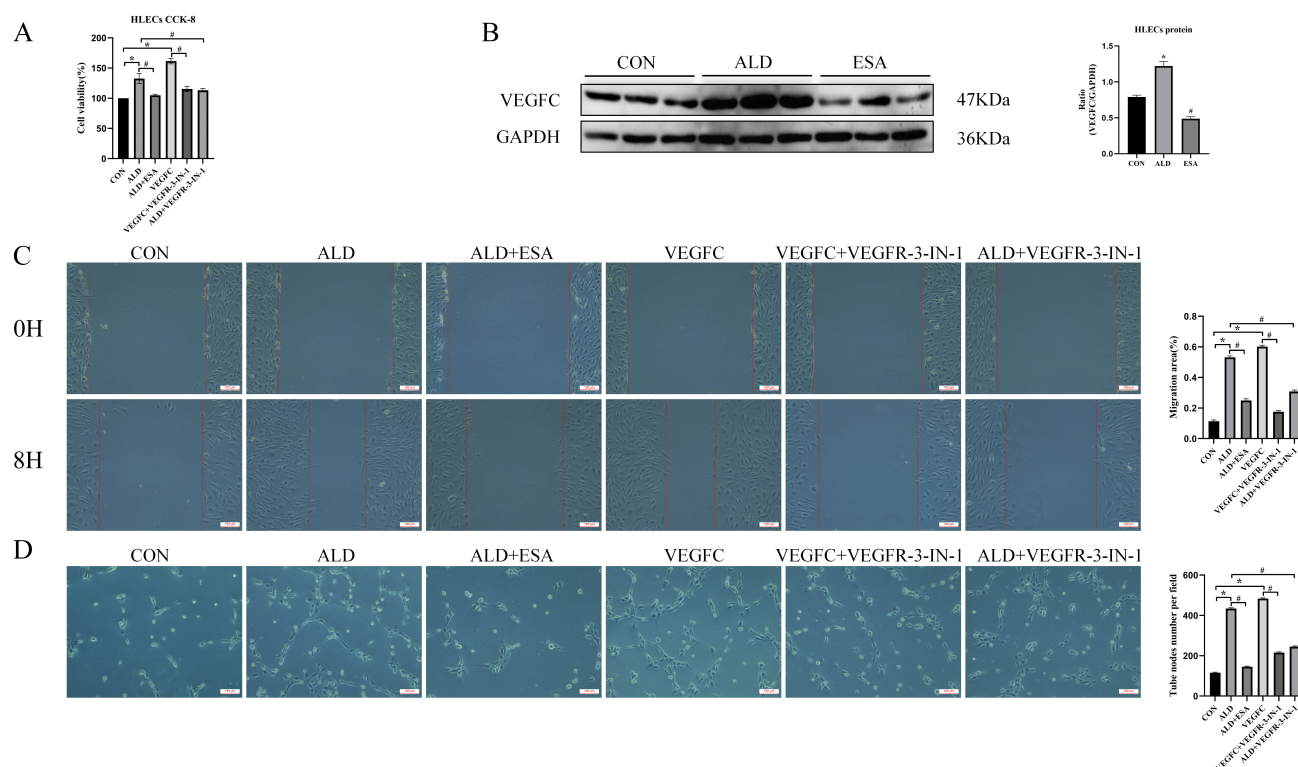


Fig. 3. Aldosterone and VEGFC promote lymphangiogenesis through mediating the proliferation, migration, and tube formation of HLECs. (A) VEGFC-induced proliferation of HLECs was determined with a CCK8 assay. (B) Western blotting was performed to analyze VEGFC expression in HLECs. (C) VEGFC promotes lymphatic vessel endothelial cell migration (scale bar = 100 μ m) and (D) tube formation (scale bar = 100 μ m). The data are expressed as the mean \pm standard deviation (n = 6). * p < 0.05 vs. the CON group, # p < 0.05 vs. the ALD/VEGFC group. HLECs, human lymphatic endothelial cells; CCK8, cell counting kit-8.

western blot. The results showed that aldosterone could up-regulate the expression of VEGFC in HLECs, and this process was inhibited by esaxerenone (Fig. 3B), further confirming that aldosterone regulated the secretion of VEGFC by HLECs through the activation of MR. In addition, aldosterone and VEGFC directly promoted the migration rate and tube formation capacity of HLECs, whereas the VEGFC inhibitors VEGFR-3-IN-1 and esaxerenone attenuated these effects (Fig. 3C,D). These findings indicated that MR/VEGFC might play a regulatory role in lymphangiogenesis.

To confirm the *in vivo* findings, an *in vitro* study was performed on aldosterone-treated RAW264.7 cells. Western blots revealed that the expression of VEGFC, TGF- β 1, TNF- α , and IL-1 β was elevated in aldosterone-treated RAW264.7 cells compared with CON (Fig. 4A). Moreover, the ELISA results for aldosterone-treated RAW264.7 cell supernatants were consistent with the above results (Fig. 4B). Aldosterone acts through MR activation [14]. Western blot analysis demonstrated that total MR expression levels were comparable among the CON, ALD, and ESA groups. However, a significant difference was observed in the nuclear expression of MR, with higher levels detected in the ALD group than in the CON group. whereas

nuclear accumulation of MR was inhibited by esaxerenone (Fig. 4A).

3.3 Aldosterone Induces EndMT In Vitro and In Vivo

EndMT is a recognized cell transdifferentiation type that has emerged as an alternative source of tissue myofibroblasts. TGF- β 1 can induce EndMT. Numerous studies have shown that EndMT is involved in the development of renal fibrosis [15]. In this study, we conducted immunofluorescence staining for LYVE-1 and vimentin in renal tissues. The number of LYVE-1⁺ vimentin⁺ cells was meaningfully increased in the kidneys of aldosterone-treated mice, and esaxerenone remarkably decreased the number of these double-positive cells (Fig. 5A). In the CON and ESA groups, we selected the locations in which LYVE-1⁺ and vimentin⁺ cells were adjacent to each other, indicating that little lymphatic endothelial cell transformation into myofibroblasts occurred in both CON group and the ESA group (Fig. 5A). We also performed immunofluorescence labeling of kidney tissues with LYVE-1 and α -SMA antibodies, and the results were consistent with those described above (Fig. 5B). Immunohistochemical staining for vimentin, α -SMA and collagen III revealed significantly greater collagen deposition in aldosterone-treated mice than

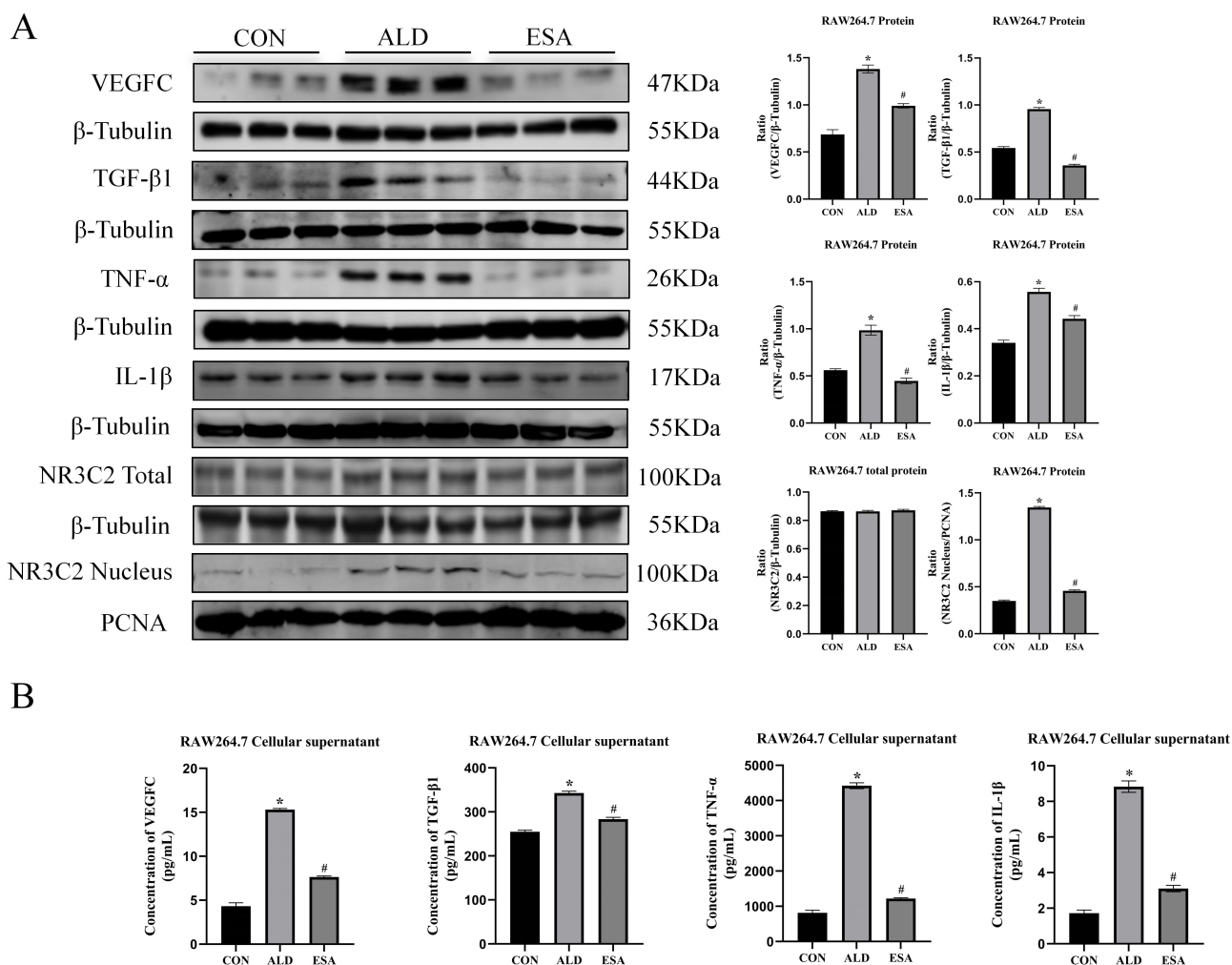


Fig. 4. Aldosterone activates MR and induces RAW264.7 to secrete inflammatory cytokines, TGF- β 1 and VEGFC. (A) Western blots for VEGFC, TGF- β 1, TNF- α , IL-1 β , and MR in the total and nuclear fractions of RAW264.7 cells. **(B)** ELISA for serum VEGFC, TGF- β 1, TNF- α , and IL-1 β protein levels in aldosterone-treated RAW264.7 cells. The data are expressed as the mean \pm standard deviation ($n = 6$). * $p < 0.05$ vs. the CON group, # $p < 0.05$ vs. the ALD group.

in control mice (Fig. 5C). Using western blot, we semi-quantified renal tissue vimentin and α -SMA expression, and the results were consistent with those of the histochemical analysis (Fig. 5D). Moreover, to elucidate the mechanism by which aldosterone promotes EndMT in HLECs, we incubated HLECs with aldosterone in the presence or absence of esaxerenone for 24 hours *in vitro*. Flow cytometry of HLECs cultured with aldosterone revealed that vimentin and α -SMA expression was significantly greater in ALD treated cells than in control cells, while the addition of the MR antagonist esaxerenone inhibited the transformation of the lymphatic endothelium into myofibroblasts (Fig. 5E). These results suggested that aldosterone promoted the transformation of lymphatic endothelial cells into myofibroblasts and that esaxerenone inhibited EndMT.

EndMT contributes to fibrosis by driving collagen production, as observed in the analysis of aldosterone-infused mouse kidneys via trichromatic confocal mi-

croscopy and Z-stacks, which revealed an increase in the coexpression of LYVE-1⁺ vimentin⁺ type III collagen cells. In contrast, the ESA group had significantly fewer co-expressing cells and significantly less fibrosis (Fig. 6A,B; **Supplementary Video**). These results suggested that collagen secretion by lymphatic endothelial cells undergoing phenotypic transformation was involved in renal fibrosis.

To further investigate the effects of aldosterone and TGF- β 1 on EndMT, we cultured HLECs with aldosterone and the antagonist esaxerenone or with TGF- β 1 and the receptor blocker LY2109761 for 24 h. Flow cytometry demonstrated that the expression of vimentin and α -SMA was upregulated in the ALD group and the TGF- β 1 group compared with the CON group. The addition of esaxerenone or LY2109761 inhibited the transformation of the lymphatic endothelium to myofibroblasts, and the number of α -SMA or vimentin positive cells in the ALD+LY2109761 group was lower than that in the

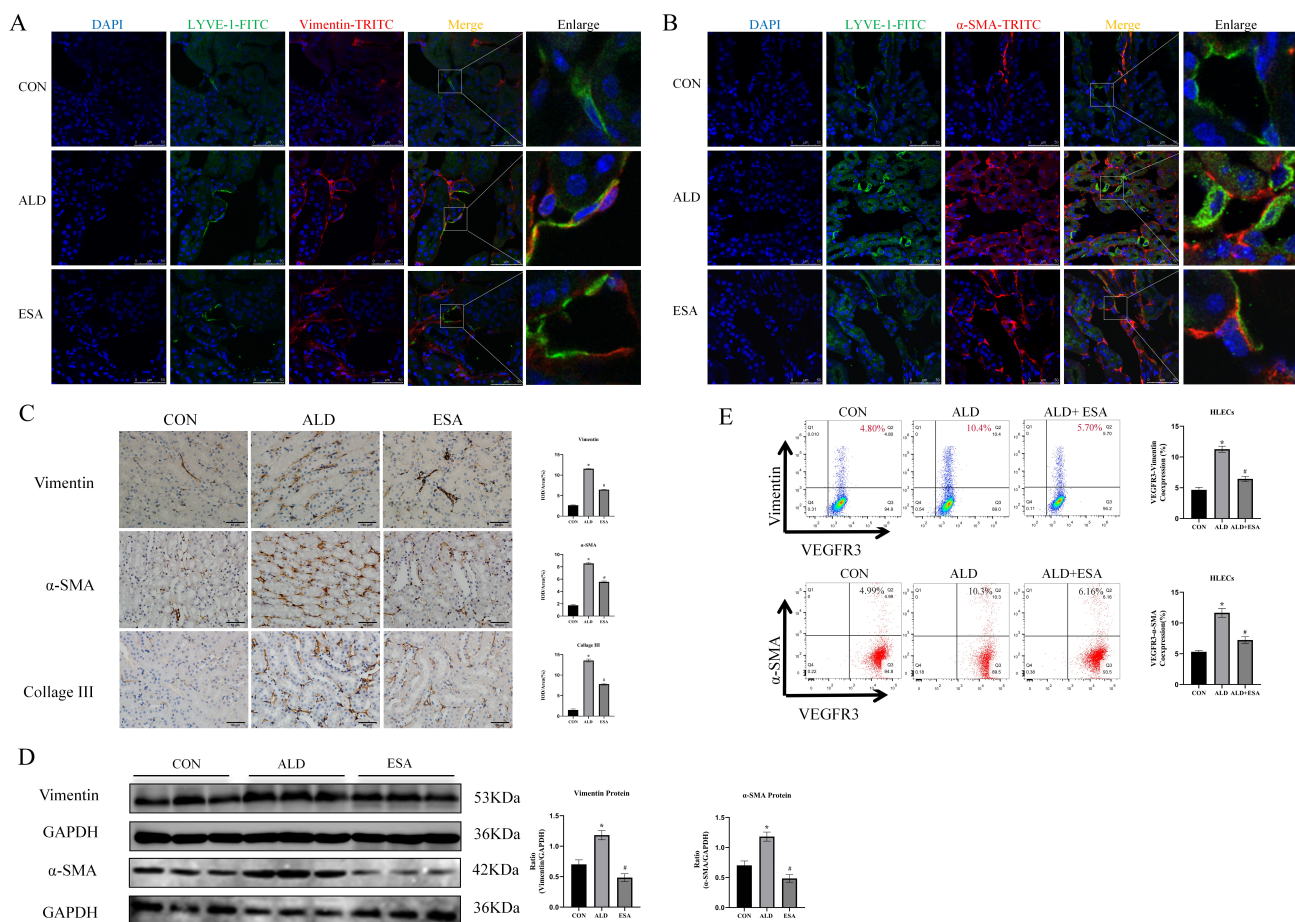
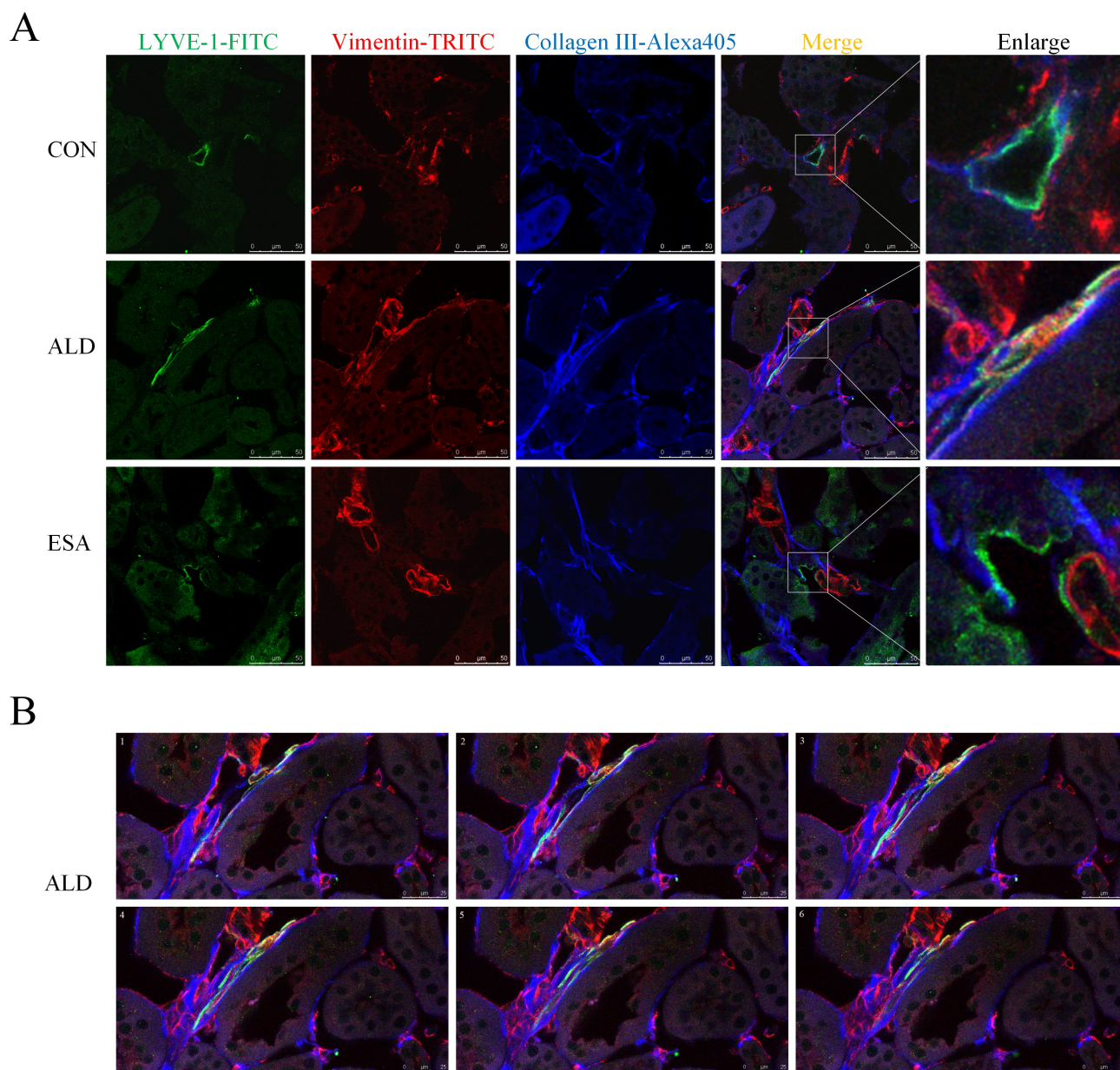


Fig. 5. Aldosterone induces EndMT in mouse kidneys and HLECs. (A) Kidney sections were immunofluorescently stained with antibodies against the lymphatic endothelial cell marker LYVE-1 (green) and the myofibroblast marker vimentin (red) to identify EndMT (cells expressing both markers indicate EndMT; nuclei (blue) were stained with DAPI) (scale bar = 50 μ m). Enlarged images showed a 5 \times magnification of the areas within the white rectangles in the merged images. (B) Kidney sections were subjected to immunofluorescence staining with LYVE-1 antibody (green) and α -SMA antibody (red) to identify EndMT (cells expressing both markers indicate EndMT; cell nuclei (blue) were stained with DAPI) (scale bar = 50 μ m). Enlarged images showed a 5 \times magnification of the areas within the white rectangles in the merged images. (C) Myofibroblastic renal infiltration and collagen deposition were examined using immunohistochemical staining for α -SMA, vimentin and collagen III (scale bar = 50 μ m). (D) Western blots for vimentin and α -SMA in kidney tissues ($n = 6$). (E) Flow cytometry analysis of vimentin and α -SMA expression in HLECs treated with ALD. Q2 indicates the percentage of vimentin⁺/ α -SMA⁺ and VEGFR3⁺ EndMT cells ($n = 3$). The data are expressed as the mean \pm standard deviation. * $p < 0.05$ vs. the CON group, # $p < 0.05$ vs. the ALD group. EndMT, endothelial-to-mesenchymal transition.

ALD group (Fig. 7A), indicating that the TGF- β 1 receptor blocker antagonized the aldosterone-induced EndMT. Semiquantitative analysis of Vimentin and α -SMA expression by western blot was performed, and the results supported the above conclusions (Fig. 7B). To further investigate whether aldosterone regulated the expression of TGF- β 1 in HLECs via MR, we detected TGF- β 1 expression in HLECs stimulated with aldosterone using western blot. The results showed that aldosterone upregulated TGF- β 1 expression in HLECs, and this effect was inhibited by esaxerenone (Supplementary Fig. 3), further confirming that aldosterone regulated TGF- β 1 expression in HLECs by activating MR.

4. Discussion

RIF which is characterized by tubulointerstitial fibrosis, is the final manifestation of a wide variety of CKD [16]. RIF is recognized as the final outcome of progressive kidney disease [17]. The impairment in renal function in end-stage renal disease is related to structural changes produced by renal fibrosis and induced by multiple vasoactive substances and cytokines, the most important of which is the renin-angiotensin-aldosterone system [18]. The protective effects of ACEIs and ARBs on the kidneys, in addition to correcting blood pressure abnormalities, include the modulation of their downstream mediator aldosterone, and the clinical effects of MRB have confirmed the criti-



Z-stack image of a EndMT cell: LYVE-1-FITC+ Vimentin-TRITC+Col-III-Alexa 405

Fig. 6. EndMT produces collagen to participate in renal fibrosis. (A) Three-color confocal microscopy images of cells coexpressing LYVE-1 (green), vimentin (red), and collagen III (blue) (scale bar = 50 μ m). Enlarged images showed a 5 \times magnification of the areas within the white rectangles in the merged images. (B) Z-stack images showing the coexpression of LYVE-1 (green), vimentin (red), and collagen III (blue) in the ALD groups (scale bar = 25 μ m) (also shown in the **Supplementary Video**).

cal role of MR activation [19]. MRBs can attenuate renal injury via pathways that include the inhibition of cell proliferation [20] and cell phenotypic transformation [8], but few studies have investigated whether MRBs reduce kidney damage by inhibiting inflammatory lymphangiogenesis induced by MR activation. In a long term (180 days) unilateral ureteral obstruction (UUO) rat model, UUO led to increases in plasma aldosterone levels, lymphangiogenesis, and myofibroblast transformation in the kidney and heart [21]. Therefore, it can be hypothesized that UUO induces

an increase in aldosterone, which in turn activates MR, induces EndMT, and promotes fibrosis. Our aldosterone-infused mice model enabled us to investigate the mechanism of aldosterone-induced inflammatory lymphangiogenesis and EndMT in renal fibrosis.

Inflammation, which involves the detection and elimination of harmful pathogens, serves as a key pathogenic mechanism in CKD [22]. While inflammation is a crucial component of the host defense system following tissue injury, persistent or unresolved inflammation contributes sig-

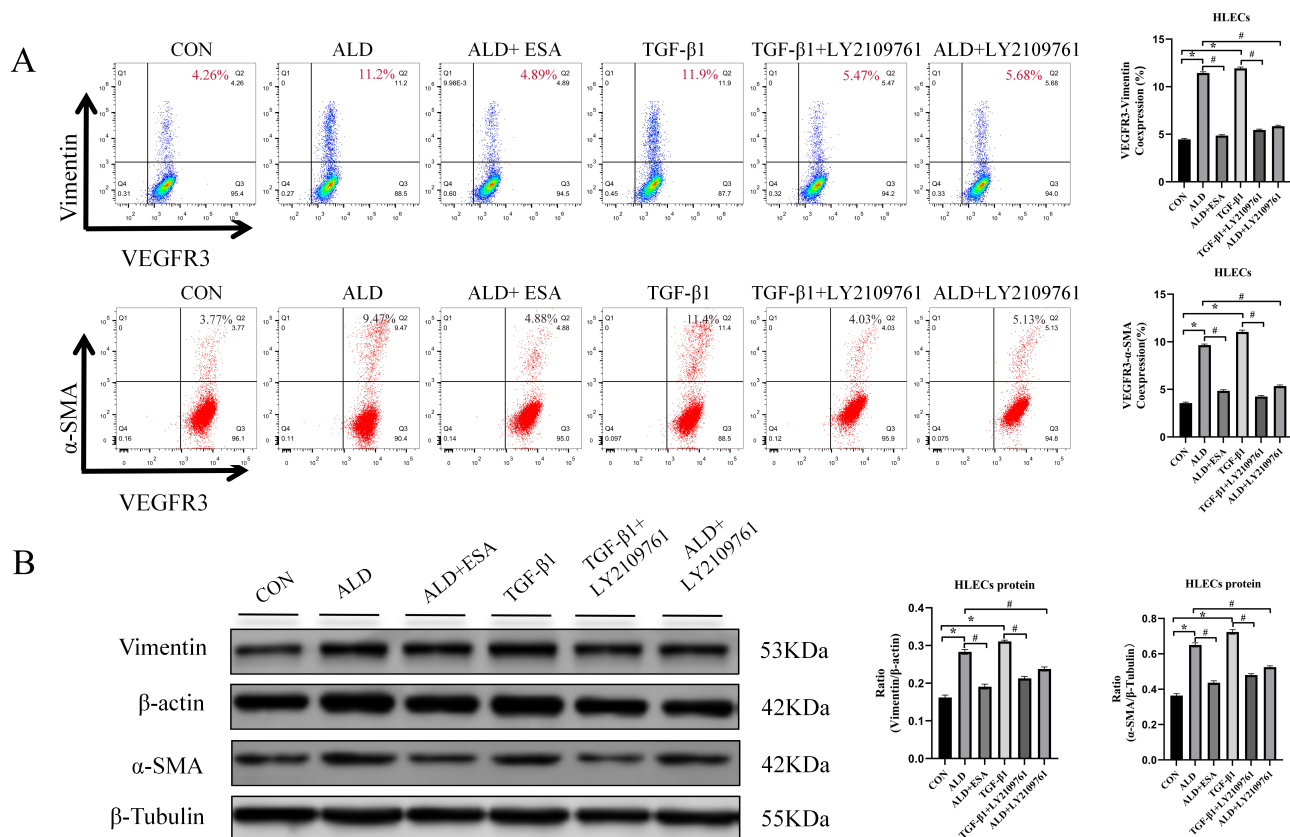


Fig. 7. Aldosterone and TGF- β 1 induce EndMT in HLECs. (A) Flow cytometry analysis of vimentin and α -SMA expression in HLECs treated with ALD and TGF- β 1; Q2 indicates the percentage of vimentin⁺/ α -SMA⁺ and VEGFR3⁺ EndMT cells (n = 3). (B) Western blots showing vimentin and α -SMA expression in HLECs (n = 3). The data are expressed as the mean \pm standard deviation. * p < 0.05 vs. the CON group, # p < 0.05 vs. the ALD/TGF- β 1 group.

nificantly to the progression of fibrotic diseases [23,24]. Furthermore, peripheral solid organ lymphangiogenesis has been implicated in a range of inflammatory conditions, such as transplant rejection, hypertension, extracellular matrix stiffness, myocardial infarction, and tumor metastasis [25–28]. We hypothesized that there was a connection between fibrotic disease and lymphangiogenesis.

The formation of new lymphatic vessels is observed in acute and chronic inflammation, tumor metastasis, and tissue or organ remodeling. However, new lymphatic vessels are poorly structured and are inadequate for the uptake of water and macromolecules and the return of lymphatic fluid, which leads to localized fluid retention [29]. The lymphatic system can be postnatally stimulated to grow and remodel. Lymphangiogenesis is often observed at sites of tissue injury, interstitial fluid overload [25], hyperglycemia [30], or inflammation and is correlated with the severity of tubulointerstitial fibrosis in many renal disorders [25]. In these settings, the extent to which this process is protective rather than maladaptive is unclear and may depend on the circumstances [31–34]. However, lymphangiogenesis can protect organs. Renal lymphangiogenesis was found to be beneficial in a UUO model at 14 days [31]. In the early

stages of renal transplantation, early restorative lymphangiogenesis reconnects the kidney to the systemic lymphatic system, and the transplant recipient may benefit from the restoration of homeostatic clearance of interstitial fluids and solutes and the clearance of infiltrating cells [35]. Whether lymphangiogenesis is beneficial or harmful to organs depends on the disease and stage. According to the results of the current study, lymphangiogenesis has a better protective effect in the early stage of ischemia and hypoxia, whereas lymphangiogenesis stimulated by chronic inflammation is involved in the formation of organ fibrosis. In this study, we detected renal lymphangiogenesis with fibrosis in aldosterone-treated mice, which warrants further study.

VEGF family members are key mediators of the growth of blood vessels and lymphatics. VEGFR3 was the first lymphospecific growth factor receptor to be identified. VEGFC and VEGFR3 are major components of the apical signaling pathway involved in the development and maintenance of lymphatic vessels [36]. The process of lymphangiogenesis includes proliferation, sprouting, migration, and vascular structure formation. VEGFC induces endothelial cell proliferation, migration, and survival [37]. In our *in vitro* experiments, we stimulated HLECs with aldosterone

and VEGFC for 24 h, and the results revealed that aldosterone and VEGFC promoted HLEC proliferation. Moreover, aldosterone and VEGFC promoted the migration of cells and the formation of tubes in HLECs, suggesting that aldosterone and VEGFC promoted the generation of lymphatic vessels. VEGFC can be secreted by a variety of renal cells and participate in lymphangiogenesis, such as tubular epithelial cells, fibroblasts and macrophages. In inflammatory injury, macrophages become the predominant source, although tubular epithelial cells also contribute to this process.

Aldosterone is a mineralocorticoid hormone that regulates fluid and electrolyte homeostasis in the body. Over the past several years, increasing evidence has demonstrated that aldosterone plays a role in activating both innate and adaptive immune cells. Specifically, macrophages and T cells respond to aldosterone by migrating to and accumulating in the kidneys, heart, and vascular system. This immune cell infiltration has been implicated in the progression of end-organ damage associated with cardiovascular and metabolic disorders [38]. Aldosterone binds to MR in local tissues and regulates target organ function. The MR activation can be verified by detecting the expression of NR3C2 in the nucleus, specifically through nuclear translocation. MR are expressed in a wide range of tissues, including smooth muscle cells, cardiomyocytes, endothelial cells, fibroblasts, macrophages, T cells and dendritic cells [39,40]. Aldosterone can induce inflammatory macrophage infiltration and the secretion of inflammatory cytokines and growth factors, which mediate inflammatory responses leading to tissue injury [13]. In our study, renal interstitial inflammatory macrophage infiltration, as well as IL-1 β , TNF- α , and TGF- β 1 expression, which were reduced by treatment with esaxerenone, increased with exposure to ALD. The main sources of VEGFC are renal tubular cells and macrophages [12,41], and we investigated whether aldosterone could increase the secretion of VEGFC by macrophages. Our results revealed that many macrophages infiltrated the renal interstitium of aldosterone-treated mice and that aldosterone promoted macrophage secretion of VEGFC. We obtained the same results *in vitro* by treating RAW264.7 macrophages with aldosterone. Notably, administration of aldosterone without a high-salt diet did not significantly alter blood pressure, yet it induced marked inflammatory injury. This was evidenced by substantial renal macrophage infiltration and concomitant renal dysfunction. These findings suggested that aldosterone-induced renal injury was mediated, at least in part, by direct proinflammatory mechanisms that were independent of elevated blood pressure.

Activated myofibroblasts are critical matrix-secreting cells in RIF and play a key role in ECM accumulation [42–44]. Myofibroblasts are a heterogeneous population that can originate from multiple sources, including epithelial cells through epithelial-to-mesenchymal transition (EMT) [45,46], EndMT [47], and local fibroblast or pericyte pro-

liferation [48]. In the aldosterone-infused mouse model of lymphatic neovascularization plus fibrosis, we investigated whether lymphatic endothelial cells transformed into myofibroblasts and led to renal fibrosis. Immunofluorescence analysis of LYVE-1⁺ vimentin⁺/ α -SMA⁺ cells revealed that compared with the CON group, the ALD group had more LYVE-1⁺ vimentin⁺/ α -SMA⁺ cells and type III collagen deposition was observed. In addition, flow cytometry was used to detect VEGFR3⁺ vimentin/ α -SMA⁺ cells *in vitro*, and the results revealed that the percentage of VEGFR3⁺ vimentin/ α -SMA⁺ double-positive cells was greater in the ALD group. Therefore, we hypothesized that nascent lymphatic endothelial cells also undergo EndMT, which is involved in the pathophysiological process of renal fibrosis.

TGF- β 1 is an important regulator of fibrosis and a potent inducer of the mesenchymal gene expression program, inducing the transformation of epithelial cells, endothelial cells, and intrinsic renal fibroblasts into myofibroblasts that express α -SMA [49]. TGF- β 1 is the main inducer of EndMT [50–55]. The flow cytometry results demonstrated that vimentin/ α -SMA expression was upregulated in the ALD group and the TGF- β 1 group with the expression levels being significantly increased compared with those in the CON group. These results verified that ALD/TGF- β 1 induced EndMT in newly formed lymphatic endothelial cells. Moreover, in HLECs *in vitro*, the TGF- β 1 receptor blocker LY2109761 alleviated TGF- β 1- and ALD-induced EndMT, suggesting that ALD could induce EndMT and promote renal fibrosis through the TGF- β 1 signaling pathway.

Lymphangiogenesis is related not only to inflammation but also to ischemia and hypoxia. In this study, we focused on lymphangiogenesis under inflammatory conditions and did not address ischemia or hypoxia. The type of macrophages from which VEGFC originates also requires further exploration. Questions for future studies include whether, in addition to promoting increased VEGFC secretion by macrophages, aldosterone also promotes VEGFC secretion by renal tubular epithelial cells and whether the macrophages promoted by aldosterone are recruited or proliferating.

This study has several limitations. First, although the main sources of VEGFC were renal tubular cells and macrophages especially those in an inflammatory injury environment, the specific types of macrophages from which VEGFC is derived have not been explored in depth, and the diversity of the sources and functions of macrophages has not been fully studied. Second, in addition to promoting the secretion of VEGFC by macrophages, aldosterone can also promote the secretion of VEGFC by renal tubular epithelial cells and other cells. The role of aldosterone in lymphangiogenesis requires more precise verification. Third, the inclusion of a separate esaxerenone treatment group would have strengthened the evidence for its direct pharmacolog-

ical effects on macrophage infiltration and VEGFC inhibition. Additionally, direct phenotypic and functional profiling of isolated renal macrophages, which would elucidate their origin, polarization state, and VEGFC secretion, was not performed. Despite these limitations, the current findings are instructive and provide a solid foundation for subsequent research endeavors.

5. Conclusions

In vivo and *in vitro* experiments demonstrated that ALD increased macrophage infiltration and activated MR in macrophages, induced the secretion of the inflammatory cytokines, VEGFC and TGF- β 1, by macrophages; and induced lymphatic vessel neogenesis. In contrast, lymphatic vessel endothelial cells were induced to transform into myofibroblasts involved in RIF via the action of TGF- β 1. The MR/ TGF- β 1 signaling pathway induced lymphangiogenesis, and new lymphatic endothelial cells underwent mesenchymal transformation and participate in RIF. Esaxerenone alleviated renal inflammation and fibrosis by suppressing the aforementioned effects. These findings indicate that modulating the MR pathway may represent a promising therapeutic strategy for the management of RIF.

Abbreviations

ALD, aldosterone; α -SMA, α smooth muscle actin; CKD, chronic kidney disease; EndMT, endothelial-to-mesenchymal transition; ESA, esaxerenone; HLECs, human lymphatic endothelial cells; MR, mineralocorticoid receptor; MRB, mineralocorticoid receptor blocker; UUO, unilateral ureteral obstruction.

Availability of Data and Materials

The original contributions presented in this study are included in the article/**Supplementary Material**. Further inquiries can be directed to the corresponding authors.

Author Contributions

Conceptualization, QYX, PPQ and TS; Methodology, LLF and ZQL; Validation, YC, XMG, JYC, FY and YZX; Formal Analysis, LLF and ZQL; Investigation, ZQL; Resources, QYX and YZX; Data Curation, LLF; Writing — Original Draft Preparation, LLF; Writing — Review & Editing, QYX, PPQ and TS; Visualization, PPQ; Supervision, QYX and TS; Project Administration, PPQ; Funding Acquisition, QYX, FY and YZX. All authors contributed to editorial changes in the manuscript. All authors read and approved the final manuscript. All authors have participated sufficiently in the work and agreed to be accountable for all aspects of the work.

Ethics Approval and Consent to Participate

The research protocol was approved by the Ethics Committee of Hebei University of Chinese Medicine (Ethic

Approval Number: No. DWLL2021063). All animal care and experimental procedures were conducted in accordance with the guidelines provided by the Animal Experimentation Ethics Committee of Hebei University of Chinese Medicine and were approved by the Animal Care and Use Committee of the same institution. All efforts were made to minimize animal distress and ensure ethical treatment.

Acknowledgment

Esaxerenone was provided by Daiichi Sankyo Co., Ltd.

Funding

This research was funded by the National Natural Science Foundation Project of China, grant number: No. 82174317; No. 82305121; No. 82205006, and the Natural Science Fund of Hebei Province, grant number: No. H2023423042.

Conflict of Interest

All authors declare no conflicts of interest. Despite Tatsuo Shimosawa received lecture honoraria from Daiichi Sankyo Co., Ltd., Esaxerenone was provided by Daiichi Sankyo Co., Ltd, the judgments in data interpretation and writing were not influenced by this relationship.

Supplementary Material

Supplementary material associated with this article can be found, in the online version, at <https://doi.org/10.31083/FBL45591>.

References

- [1] Chen TK, Knicely DH, Grams ME. Chronic Kidney Disease Diagnosis and Management: A Review. *JAMA*. 2019; 322: 1294–1304. <https://doi.org/10.1001/jama.2019.14745>.
- [2] Yuan Q, Tang B, Zhang C. Signaling pathways of chronic kidney diseases, implications for therapeutics. *Signal Transduction and Targeted Therapy*. 2022; 7: 182. <https://doi.org/10.1038/s41392-022-01036-5>.
- [3] Kerjaschki D, Regele HM, Moosberger I, Nagy-Bojarski K, Watschinger B, Soleiman A, *et al.* Lymphatic neoangiogenesis in human kidney transplants is associated with immunologically active lymphocytic infiltrates. *Journal of the American Society of Nephrology: JASN*. 2004; 15: 603–612. <https://doi.org/10.1097/01.asn.0000113316.52371.2e>.
- [4] Sakamoto I, Ito Y, Mizuno M, Suzuki Y, Sawai A, Tanaka A, *et al.* Lymphatic vessels develop during tubulointerstitial fibrosis. *Kidney International*. 2009; 75: 828–838. <https://doi.org/10.1038/ki.2008.661>.
- [5] Hao J, Qiang P, Fan L, Xiong Y, Chang Y, Yang F, *et al.* Eplerenone reduces lymphangiogenesis in the contralateral kidneys of UUO rats. *Scientific Reports*. 2024; 14: 9976. <https://doi.org/10.1038/s41598-024-60636-z>.
- [6] Deng H, Zhang J, Wu F, Wei F, Han W, Xu X, *et al.* Current Status of Lymphangiogenesis: Molecular Mechanism, Immune Tolerance, and Application Prospect. *Cancers*. 2023; 15: 1169. <https://doi.org/10.3390/cancers15041169>.
- [7] Epstein M. Aldosterone and Mineralocorticoid Receptor Signal-

- ing as Determinants of Cardiovascular and Renal Injury: From Hans Selye to the Present. *American Journal of Nephrology*. 2021; 52: 209–216. <https://doi.org/10.1159/000515622>.
- [8] Gao X, Chang J, Chang Y, Fan L, Liu Z, Zhang C, *et al.* Esaxerenone Inhibits Renal Angiogenesis and Endothelial-Mesenchymal Transition via the VEGFA and TGF- β 1 Pathways in Aldosterone-Infused Mice. *International Journal of Molecular Sciences*. 2023; 24: 11766. <https://doi.org/10.3390/ijms241411766>.
 - [9] Xiong Y, Chang Y, Hao J, Zhang C, Yang F, Wang Z, *et al.* Eplerenone Attenuates Fibrosis in the Contralateral Kidney of UUO Rats by Preventing Macrophage-to-Myofibroblast Transition. *Frontiers in Pharmacology*. 2021; 12: 620433. <https://doi.org/10.3389/fphar.2021.620433>.
 - [10] Qiang P, Hao J, Yang F, Han Y, Chang Y, Xian Y, *et al.* Esaxerenone inhibits the macrophage-to-myofibroblast transition through mineralocorticoid receptor/TGF- β 1 pathway in mice induced with aldosterone. *Frontiers in Immunology*. 2022; 13: 948658. <https://doi.org/10.3389/fimmu.2022.948658>.
 - [11] Kajiya K, Hirakawa S, Detmar M. Vascular endothelial growth factor-A mediates ultraviolet B-induced impairment of lymphatic vessel function. *The American Journal of Pathology*. 2006; 169: 1496–1503. <https://doi.org/10.2353/ajpath.2006.060197>.
 - [12] Suzuki Y, Ito Y, Mizuno M, Kinashi H, Sawai A, Noda Y, *et al.* Transforming growth factor- β induces vascular endothelial growth factor-C expression leading to lymphangiogenesis in rat unilateral ureteral obstruction. *Kidney International*. 2012; 81: 865–879. <https://doi.org/10.1038/ki.2011.464>.
 - [13] Martín-Fernández B, Rubio-Navarro A, Cortegano I, Ballesteros S, Alía M, Cannata-Ortiz P, *et al.* Aldosterone Induces Renal Fibrosis and Inflammatory M1-Macrophage Subtype via Mineralocorticoid Receptor in Rats. *PloS One*. 2016; 11: e0145946. <https://doi.org/10.1371/journal.pone.0145946>.
 - [14] Yang F, Chang Y, Zhang C, Xiong Y, Wang X, Ma X, *et al.* UUO induces lung fibrosis with macrophage-myofibroblast transition in rats. *International Immunopharmacology*. 2021; 93: 107396. <https://doi.org/10.1016/j.intimp.2021.107396>.
 - [15] Piera-Velázquez S, Li Z, Jimenez SA. Role of endothelial-mesenchymal transition (EndoMT) in the pathogenesis of fibrotic disorders. *The American Journal of Pathology*. 2011; 179: 1074–1080. <https://doi.org/10.1016/j.ajpath.2011.06.001>.
 - [16] Liu Y. Renal fibrosis: new insights into the pathogenesis and therapeutics. *Kidney International*. 2006; 69: 213–217. <https://doi.org/10.1038/sj.ki.5000054>.
 - [17] Liu Y. Cellular and molecular mechanisms of renal fibrosis. *Nature Reviews. Nephrology*. 2011; 7: 684–696. <https://doi.org/10.1038/nrneph.2011.149>.
 - [18] Lee SY, Kim SI, Choi ME. Therapeutic targets for treating fibrotic kidney diseases. *Translational Research: the Journal of Laboratory and Clinical Medicine*. 2015; 165: 512–530. <https://doi.org/10.1016/j.trsl.2014.07.010>.
 - [19] Toto RD. Aldosterone blockade in chronic kidney disease: can it improve outcome? *Current Opinion in Nephrology and Hypertension*. 2010; 19: 444–449. <https://doi.org/10.1097/MNH.0b013e32833ce6d5>.
 - [20] Fourkoti VG, Hanslik G, Hanusch F, Lepenies J, Quinkler M. Aldosterone and the kidney. *Hormone and Metabolic Research = Hormon- Und Stoffwechselforschung = Hormones et Metabolisme*. 2012; 44: 194–201. <https://doi.org/10.1055/s-0031-1295461>.
 - [21] Chen G, Chang Y, Xiong Y, Hao J, Liu L, Liu Z, *et al.* Eplerenone inhibits UUO-induced lymphangiogenesis and cardiac fibrosis by attenuating inflammatory injury. *International Immunopharmacology*. 2022; 108: 108759. <https://doi.org/10.1016/j.intimp.2022.108759>.
 - [22] Andrade-Oliveira V, Foresto-Neto O, Watanabe IKM, Zatz R, Câmara NOS. Inflammation in Renal Diseases: New and Old Players. *Frontiers in Pharmacology*. 2019; 10: 1192. <https://doi.org/10.3389/fphar.2019.01192>.
 - [23] Schroder K, Tschopp J. The inflammasomes. *Cell*. 2010; 140: 821–832. <https://doi.org/10.1016/j.cell.2010.01.040>.
 - [24] Nathan C, Ding A. Nonresolving inflammation. *Cell*. 2010; 140: 871–882. <https://doi.org/10.1016/j.cell.2010.02.029>.
 - [25] Machnik A, Neuhofer W, Jantsch J, Dahlmann A, Tammela T, Machura K, *et al.* Macrophages regulate salt-dependent volume and blood pressure by a vascular endothelial growth factor-C-dependent buffering mechanism. *Nature Medicine*. 2009; 15: 545–552. <https://doi.org/10.1038/nm.1960>.
 - [26] Frye M, Taddei A, Dierkes C, Martinez-Corral I, Fielden M, Orstäter H, *et al.* Matrix stiffness controls lymphatic vessel formation through regulation of a GATA2-dependent transcriptional program. *Nature Communications*. 2018; 9: 1511. <https://doi.org/10.1038/s41467-018-03959-6>.
 - [27] Henri O, Poueche C, Houssari M, Galas L, Nicol L, Edwards-Lévy F, *et al.* Selective Stimulation of Cardiac Lymphangiogenesis Reduces Myocardial Edema and Fibrosis Leading to Improved Cardiac Function Following Myocardial Infarction. *Circulation*. 2016; 133: 1484–1497; discussion 1497. <https://doi.org/10.1161/CIRCULATIONAHA.115.020143>.
 - [28] Ma Q, Dieterich LC, Detmar M. Multiple roles of lymphatic vessels in tumor progression. *Current Opinion in Immunology*. 2018; 53: 7–12. <https://doi.org/10.1016/j.coi.2018.03.018>.
 - [29] Nykänen AI, Sandelin H, Krebs R, Keränen MAI, Tuuminen R, Kärpänen T, *et al.* Targeting lymphatic vessel activation and CCL21 production by vascular endothelial growth factor receptor-3 inhibition has novel immunomodulatory and antiarteriosclerotic effects in cardiac allografts. *Circulation*. 2010; 121: 1413–1422. <https://doi.org/10.1161/CIRCULATIONAHA.109.910703>.
 - [30] Choi SY, Lim SW, Salimi S, Yoo EJ, Lee-Kwon W, Lee HH, *et al.* Tonicity-Responsive Enhancer-Binding Protein Mediates Hyperglycemia-Induced Inflammation and Vascular and Renal Injury. *Journal of the American Society of Nephrology: JASN*. 2018; 29: 492–504. <https://doi.org/10.1681/ASN.2017070718>.
 - [31] Hasegawa S, Nakano T, Torisu K, Tsuchimoto A, Eriguchi M, Haruyama N, *et al.* Vascular endothelial growth factor-C ameliorates renal interstitial fibrosis through lymphangiogenesis in mouse unilateral ureteral obstruction. *Laboratory Investigation; a Journal of Technical Methods and Pathology*. 2017; 97: 1439–1452. <https://doi.org/10.1038/labinvest.2017.77>.
 - [32] Hwang SD, Song JH, Kim Y, Lim JH, Kim MY, Kim EN, *et al.* Inhibition of lymphatic proliferation by the selective VEGFR-3 inhibitor SAR131675 ameliorates diabetic nephropathy in db/db mice. *Cell Death & Disease*. 2019; 10: 219. <https://doi.org/10.1038/s41419-019-1436-1>.
 - [33] Huang JL, Woolf AS, Kolatsi-Joannou M, Baluk P, Sandford RN, Peters DJM, *et al.* Vascular Endothelial Growth Factor C for Polycystic Kidney Diseases. *Journal of the American Society of Nephrology: JASN*. 2016; 27: 69–77. <https://doi.org/10.1681/ASN.2014090856>.
 - [34] Zarjou A, Black LM, Bolisetty S, Traylor AM, Bowhay SA, Zhang MZ, *et al.* Dynamic signature of lymphangiogenesis during acute kidney injury and chronic kidney disease. *Laboratory Investigation; a Journal of Technical Methods and Pathology*. 2019; 99: 1376–1388. <https://doi.org/10.1038/s41374-019-0259-0>.
 - [35] Vass DG, Hughes J, Marson LP. Restorative and rejection-associated lymphangiogenesis after renal transplantation: friend or foe? *Transplantation*. 2009; 88: 1237–1239. <https://doi.org/10.1097/TP.0b013e3283181c1afa7>.
 - [36] Zhang L, Zhou F, Han W, Shen B, Luo J, Shibuya M, *et*

- al.* VEGFR-3 ligand-binding and kinase activity are required for lymphangiogenesis but not for angiogenesis. *Cell Research*. 2010; 20: 1319–1331. <https://doi.org/10.1038/cr.2010.116>.
- [37] Tammela T, Enholm B, Alitalo K, Paavonen K. The biology of vascular endothelial growth factors. *Cardiovascular Research*. 2005; 65: 550–563. <https://doi.org/10.1016/j.cardiores.2004.12.002>.
- [38] Ferreira NS, Tostes RC, Paradis P, Schiffrin EL. Aldosterone, Inflammation, Immune System, and Hypertension. *American Journal of Hypertension*. 2021; 34: 15–27. <https://doi.org/10.1093/ajh/hpaa137>.
- [39] Barrera-Chimal J, Bonnard B, Jaisser F. Roles of Mineralocorticoid Receptors in Cardiovascular and Cardiorenal Diseases. *Annual Review of Physiology*. 2022; 84: 585–610. <https://doi.org/10.1146/annurev-physiol-060821-013950>.
- [40] Jaisser F, Farman N. Emerging Roles of the Mineralocorticoid Receptor in Pathology: Toward New Paradigms in Clinical Pharmacology. *Pharmacological Reviews*. 2016; 68: 49–75. <https://doi.org/10.1124/pr.115.011106>.
- [41] Lee AS, Lee JE, Jung YJ, Kim DH, Kang KP, Lee S, *et al.* Vascular endothelial growth factor-C and -D are involved in lymphangiogenesis in mouse unilateral ureteral obstruction. *Kidney International*. 2013; 83: 50–62. <https://doi.org/10.1038/ki.2012.312>.
- [42] Liu B, Jiang J, Liang H, Xiao P, Lai X, Nie J, *et al.* Natural killer T cell/IL-4 signaling promotes bone marrow-derived fibroblast activation and M2 macrophage-to-myofibroblast transition in renal fibrosis. *International Immunopharmacology*. 2021; 98: 107907. <https://doi.org/10.1016/j.intimp.2021.107907>.
- [43] Feng YL, Wang WB, Ning Y, Chen H, Liu P. Small molecules against the origin and activation of myofibroblast for renal interstitial fibrosis therapy. *Biomedicine & Pharmacotherapy = Biomedecine & Pharmacotherapie*. 2021; 139: 111386. <https://doi.org/10.1016/j.biopha.2021.111386>.
- [44] Djurdjaj S, Boor P. Cellular and molecular mechanisms of kidney fibrosis. *Molecular Aspects of Medicine*. 2019; 65: 16–36. <https://doi.org/10.1016/j.mam.2018.06.002>.
- [45] Li L, Xu L, Wen S, Yang Y, Li X, Fan Q. The effect of lncRNA-ARAP1-AS2/ARAP1 on high glucose-induced cytoskeleton rearrangement and epithelial-mesenchymal transition in human renal tubular epithelial cells. *Journal of Cellular Physiology*. 2020; 235: 5787–5795. <https://doi.org/10.1002/jcp.29512>.
- [46] Kriz W, Kaissling B, Le Hir M. Epithelial-mesenchymal transition (EMT) in kidney fibrosis: fact or fantasy? *The Journal of Clinical Investigation*. 2011; 121: 468–474. <https://doi.org/10.1172/jci44595>.
- [47] Lovisa S, Fletcher-Sanankone E, Sugimoto H, Hensel J, Lahiri S, Hertig A, *et al.* Endothelial-to-mesenchymal transition compromises vascular integrity to induce Myc-mediated metabolic reprogramming in kidney fibrosis. *Science Signaling*. 2020; 13: eaaz2597. <https://doi.org/10.1126/scisignal.aaz2597>.
- [48] Falke LL, Gholizadeh S, Goldschmeding R, Kok RJ, Nguyen TQ. Diverse origins of the myofibroblast—implications for kidney fibrosis. *Nature Reviews. Nephrology*. 2015; 11: 233–244. <https://doi.org/10.1038/nrneph.2014.246>.
- [49] Mack M, Yanagita M. Origin of myofibroblasts and cellular events triggering fibrosis. *Kidney International*. 2015; 87: 297–307. <https://doi.org/10.1038/ki.2014.287>.
- [50] Arciniegas E, Sutton AB, Allen TD, Schor AM. Transforming growth factor beta 1 promotes the differentiation of endothelial cells into smooth muscle-like cells in vitro. *Journal of Cell Science*. 1992; 103 (Pt 2): 521–529. <https://doi.org/10.1242/jcs.103.2.521>.
- [51] Goumans MJ, van Zonneveld AJ, ten Dijke P. Transforming growth factor beta-induced endothelial-to-mesenchymal transition: a switch to cardiac fibrosis? *Trends in Cardiovascular Medicine*. 2008; 18: 293–298. <https://doi.org/10.1016/j.tcm.2009.01.001>.
- [52] Markwald RR, Fitzharris TP, Manasek FJ. Structural development of endocardial cushions. *The American Journal of Anatomy*. 1977; 148: 85–119. <https://doi.org/10.1002/aja.1001480108>.
- [53] Mihira H, Suzuki HI, Akatsu Y, Yoshimatsu Y, Igarashi T, Miyazono K, *et al.* TGF- β -induced mesenchymal transition of MS-1 endothelial cells requires Smad-dependent cooperative activation of Rho signals and MRTF-A. *Journal of Biochemistry*. 2012; 151: 145–156. <https://doi.org/10.1093/jb/mvr121>.
- [54] van Meeteren LA, ten Dijke P. Regulation of endothelial cell plasticity by TGF- β . *Cell and Tissue Research*. 2012; 347: 177–186. <https://doi.org/10.1007/s00441-011-1222-6>.
- [55] Xiao L, Dudley AC. Fine-tuning vascular fate during endothelial-mesenchymal transition. *The Journal of Pathology*. 2017; 241: 25–35. <https://doi.org/10.1002/path.4814>.